JOURNAL OF CATALYSIS 63, 271–284 (1980)

V_2O_5–K_2SO_4–Silica System: The Structure and Activity of Silica-Supported V_2O_5–K_2SO_4 Catalysts

R. K. SHARMA, K. N. RAI,[1] AND R. D. SRIVASTAVA[2]

Department of Chemical Engineering, Indian Institute of Technology, Kanpur-208016, India

Received April 12, 1979; revised November 1, 1979

Silica-supported V_2O_5–K_2SO_4 catalysts containing up to 70 wt% of the total active phase, calcined at 550°C for 6 hr, have been studied by means of electron microscopy, DTA, TGA, X-ray, and BET studies. The correlation of measured physicochemical properties with the catalytic activity for methanol oxidation was investigated. X-Ray and electron microscope observations have indicated the presence of V_2O_5–K_2SO_4 in all the catalyst samples without any interaction between them. The results of the thermal analyses showed that K_2SO_4 was not dissolved in the V_2O_5 matrix. Electron microscopy indicated the presence of needle-type V_2O_5 crystals. These needle structures, which depend on K_2SO_4 concentration, appear to be more active for the methanol oxidation. The values of average pore radius and surface area simultaneously play an important role in the activity of the catalyst. Electron microscopy and X-ray analysis of a spent catalyst showed that the fundamental components of the fresh catalyst were completely retained. However, the needle structures and other large particles partially disintegrated during catalysis over extended runs.

INTRODUCTION

Pure V_2O_5 has for a long time been one of the best oxidation catalysts for a number of reactions like those of SO_2 (*1–4*), methanol (*5*), toluene (*6*), benzene (*7*), and propylene (*8*). In addition to some metal oxides such as Fe_2O_3, Co_3O_4, NiO, and MoO_3 (*9, 10*), alkali metal sulphates (*11–19*) have also been found to influence the catalytic activity of V_2O_5 and their promoting action was found to increase from Li_2SO_4 to Cs_2SO_4. Among these sulphates K_2SO_4 was reported to be the best promoter.

Though pure V_2O_5 and systems like V_2O_5–Fe_2O_3 have been examined by some workers (*20–22*), only a few investigations into the structural properties of the V_2O_5–K_2SO_4 catalyst system have been reported. Kiyoura (*23*), in his studies on V_2O_5–K_2SO_4 melt, presented the "molten state theory" for the promotive action of K_2SO_4. Trama *et al.* (*24*) in their studies on the V_2O_5–K_2SO_4–kieselguhr system found that the catalyst gave an ESR spectrum similar to that of the V_2O_5–$K_2S_2O_7$ catalyst. Later on Trama *et al.* (*25*) investigated the structural properties of V_2O_5–K_2SO_4 melt using X-ray, ESR, infrared, and magnetic susceptibility measurements and made an attempt to correlate these physicochemical properties with the catalytic activity for CO oxidation. Recently, Hassan and Iskandar (*26*) investigated the catalytic and surface characteristics of fresh, exhausted, and regenerated commercial V_2O_5–K_2SO_4–silica catalyst. The surface characteristics were studied by using X-ray, electron microscopy, and BET measurements. Their studies were limited to a single catalyst composition.

From the literature review, it is evident that there has been no prior detailed study on the structure of the supported V_2O_5–K_2SO_4 catalyst system. Search of suitable model reactions has indicated a variety of interesting cases which will constitute the

[1] Present address: Department of Metallurgical Engineering and Materials Science, Indian Institute of Technology, Kanpur-208016, India.

[2] To whom queries concerning this paper should be sent.

0021-9517/80/060271-14$02.00/0

basis of future papers: among them, for the present paper, we have chosen the methanol oxidation reaction for investigating the activity of the catalyst.

In the present work, results of solid-state properties of a series of silica-supported V_2O_5–K_2SO_4 catalysts using electron microscopy, DTA, TGA, X-ray, and BET studies are presented and correlated with the catalytic activity for the methanol oxidation. Studies of this type are expected to lead to a better understanding of the nature of catalysts in relation to the activity.

EXPERMENTAL

Preparation of the Samples

V_2O_5 was prepared by the calcination of ammonium metavanadate at 450°C for 4 hr. A series of silica-supported catalysts containing about 25 to 70 wt% active phase was prepared by the impregnation technique. The impregnate was vacuum dried at 70°C and then calcined at 550°C for 6 hr. K_2SO_4 content in all the nine samples of the series ranged from 10 to 20%.

Reference to various samples will be made giving their composition as weight percent V_2O_5 and K_2SO_4. Hence, V-20–K-15 means a sample of V_2O_5–K_2SO_4 supported on silica having 20% of the active element as V_2O_5, 15% of the promoter as K_2SO_4, and the balance as silica.

Physicochemical Characterization

The catalysts were characterized by X-ray, DTA, TGA, electron microscopy, and BET studies. The experimental apparatus, procedures, and conditions of experiments were similar to those used by Athappan (*27*) in the characterization of the NiO–Al_2O_3 system, and only a brief description is given here.

X-Ray powder analysis. X-Ray powder diffraction spectra were obtained at room temperature using a General Electronic diffractometer with nickel filtered CuKα radiation. The diffractometer was operated with 2° diverging and receiving slits at a scan rate of 1°/min and a continuous trace of intensity as a function of 2θ was recorded. Spectra of finely ground samples were run in the 2θ range of 0–80°.

DTA and TGA. Differential thermal analysis (DTA) and thermogravimetric analysis (TGA) of the samples were carried out simultaneously using a complex thermoanalytical equipment (Derivatograph, M.O.M. Budapest). α-Al_2O_3 was used as a reference material.

Surface area and pore volume. Surface areas of the catalysts were calculated from N_2 adsorption isotherms using BET apparatus. Pore volume and pore size distribution were measured by a mercury porosimeter.

Electron microscopy. The Phillips E.M. 301 electron microscope excited at 80 kV with a eugocentic goniometer at a resolution better than 10 Å was used during this investigation. The magnification and rotation calibrations were carried out by standard procedures. The diffraction camera constant λL was calibrated for 80 kV at a particular lens setting using (111), (200), (220), and (311) diffraction lines from evaporated pure-gold film. The catalyst particles were supported on the carbon-coated copper support grids from a methyl alcohol suspension.

Catalytic Activity

The activity of the catalyst was studied using methanol oxidation as the test reaction. The details of the experimental apparatus, procedures, and analytical techniques have been described previously (*19*). The product analysis indicated that there was always some amount of unreacted methanol present.

RESULTS AND DISCUSSION

A. Physicochemical Characterization

1. X-Ray Diffraction

The diffraction pattern of vanadium oxides prepared from ammonium metavana-

date was indexicle on the basis of the V_2O_5 orthorhombic cell (a = 11.51 Å, b = 3.559 Å, and c = 4.37 Å). For all the catalyst samples examined, the X-ray diffraction revealed the presence of both V_2O_5 (orthorhombic cell) and K_2SO_4 (hexagonal cell, a = 5.71 Å and c = 7.86 Å). The maximum intensity line was always at 2θ = 31.2° (d = 2.86 Å). There was an indication that as the concentration of K_2SO_4 in the sample decreases, the intensity of the line at the corresponding 2θ values 21.2° (d = 4.19 Å), 29.9° (d = 3.09 Å), and 43.0° (d = 2.10 Å) decreases. Similarly, the intensity of the line at the corresponding 2θ values of 15.4° (d = 5.76 Å), 20.2° (d = 4.38 Å), and 26.16° (d = 3.40 Å) decreases with the decrease in V_2O_5 concentration.

Trama *et al.* (*25*) and Hassan and Iskandar (*26*) have studied this catalyst which was prepared at 700°C. If X-ray diffraction results for pure V_2O_5 and the catalyst samples are compared to those of V_5O_9 (*26*), the absence of the diffraction bands corresponding to 2θ values of 22.1° (d = 3.97 Å) and 26.8° (d = 3.32 Å) indicates a lack in the formation of V_5O_9 under the present conditions of the system studied. The interaction products $VOSO_4$ (*25*) and 4 $V_2O_5 \cdot K_2O$ (*28*) reported earlier in the catalyst melt at 700°C were found to be absent in the present studies. Although the evidence for the presence of the above interaction products is not easily offered by X-ray techniques alone, electron microscopy has also supported their absence. The results of the electron microscope studies are described later.

2. *DTA and TGA*

DTA of ammonium metavanadate, used in the preparation of V_2O_5, has shown two sharp endotherms at 250 and 690°C, indicating that decomposition of ammonium metavanadate to V_2O_5 is complete at 250°C. This was also verified by the observed weight loss of about 25% by TGA. This V_2O_5 so formed melts at 690°C. It is in agreement with the results obtained for pure V_2O_5, where only one endotherm at 690°C was obtained. Except for an endothermal transformation at 550°C, DTA of K_2SO_4 did not show any other transformation till 1000°C. This endotherm may be attributed to the phase transformation of rhombic crystals of K_2SO_4, which may be present, to hexagonal structure (*31*). TGA only showed a gradual loss in weight up to 150°C due to the loss of atmospheric water of hydration.

DTA of all the catalyst samples calcined at 550°C for 6 hr has shown one small endotherm at 690°C. Besides, a small drift in the baseline up to 150°C was also observed. The transformation at 690°C may be attributed to the melting of V_2O_5 present in the specimen. With these catalysts, the TGA experiments showed only a gradual change in weight up to 150°C.

3. *BET Analysis*

Compositions of the catalysts and their specific surface area, pore volume, porosity, pore size distribution, and the calculated values of mean pore radius ($\bar{r} = 2 V_p/S.A.$) are summarized in Table 1. The surface area of the original silica support was 74.6 m^2/g. An examination of the table shows that the surface area passes through a minimum as K_2SO_4 concentration in the catalyst increases. It seems some very small crystals of K_2SO_4 are formed when K_2SO_4 concentration exceeds a certain value, resulting in an increase in the surface area. This will lower the calculated values of pore radii. Also, at these compositions more micropores are possibly formed than are originally present in the support, resulting in a further decrease of pore radii.

4. *Electron Microscopy*

The transmission electron microscopy was carried out to study the structure and state of dispersion of the active components on the silica support, to estimate the particle size distribution for the active

TABLE 1

Physical Characteristics of V_2O_5–K_2SO_4–Silica Catalysts

Catalyst	Surface area (m^2/g)	Pore volume (cm^3/g)	Porosity, ($cm^3/100\ cm^3$)	Average pore radius (Å)	Pore size distribution(Å)						
					4–60	60–100	100–200	200–300	300–400	400–500	500–75000
V-20–K-20	18.00	0.2821	39.7	313.4	0.0	0.7	0.7	0.3	1.5	11.4	85.4
V-20–K-15	5.20	0.3030	41.7	1165.3	0.0	0.6	0.6	0.4	0.8	8.3	89.3
V-20–K-10	2.80	0.3588	45.1	2562.8	0.0	0.6	0.5	0.6	0.6	5.7	92.1
V-20–K-5	8.20	0.4186	49.6	1020.9	0.0	0.0	0.9	1.1	6.2	21.1	70.7
V-15–K-20	16.00	0.3352	43.2	419.0	0.0	0.3	0.6	1.6	10.7	27.9	58.9
V-15–K-15	9.80	0.3555	44.4	725.5	0.0	0.2	0.4	0.9	6.2	19.8	72.5
V-15–K-10	7.00	0.4060	47.7	1160.0	0.0	0.3	0.2	0.3	1.3	11.1	86.8
V-15–K-5	12.20	0.4791	53.2	785.4	0.0	0.0	0.5	1.1	8.9	33.4	56.1
V-10–K-20	30.80	0.3990	49.8	259.0	2.4	1.6	1.2	4.6	18.2	24.5	47.5
V-10–K-15	17.30	0.4207	50.3	486.3	1.8	1.5	2.5	5.4	16.2	28.8	43.8
V-10–K-10	13.00	0.4527	51.8	696.4	3.6	1.0	3.10	9.8	19.7	24.8	38.0
V-10–K-5	19.40	0.5068	54.3	522.4	0.0	0.0	0.0	4.2	12.1	30.9	52.8

phase and the support, and to study any chemical interaction between the catalyst constituents.

Figure 1a shows the electron micrograph of a sample of V-20–K-15 catalyst. In addition to small particles of V_2O_5 and K_2SO_4 on silica, some needle-type crystals are also observed. The electron diffraction pattern from these needles is shown in Fig. 1b. The pattern was indexicle on the basis of V_2O_5 structure (orthorhombic cell, a = 11.60 Å, b = 3.556 Å, and c = 4.37 Å). It is not clear as to how and which stage of catalyst preparation these needles have formed. However, their proportion is not the same in all the catalyst samples. Except small particles and these needle-type structures, no other form of V_2O_5 was detected. Hassan and Iskandar (*26*) have also shown the presence of such needles in their studies on the commercial V-10–K-10 catalyst. In the absence of diffraction studies, it was not possible for them to identify these needles. Similarly, in all the catalyst samples, very thin platelet-shaped crystals as shown in Fig. 2a were observed. The diffraction pattern from such platelets (Fig. 2b) corresponded to K_2SO_4 structure (hexagonal cell, a = 5.71 Å and b = 7.85 Å).

Figure 3a shows the electron micrograph of V-20–K-10 grain. V_2O_5 and K_2SO_4 particles are seen to coat the silica particles smoothly. It is difficult to resolve the isolated active-phase particles due to the crowding since they appear to have formed a thick continuous layer over the support. The individual active-phase particles finely dispersed over the support are clearly visible in Fig. 3b. In general, V_2O_5 and K_2SO_4 appear to be completely intermixed and it is difficult to isolate them on electron micrographs from their image contrast. The particle size distribution of V_2O_5 and K_2SO_4 determined from Fig. 3b indicate an average particle size of 60 Å for these V_2O_5 and K_2SO_4 particles. It is to be noted from the pore size distribution data (Table 1) that a majority of the pores of the catalyst are greater than 60 Å. It is thus possible that most of the micropores are filled with the active phase, resulting in a loss of physical surface area. This may be the possible explanation for the low values of the physical surface area of the samples. The large values of the pore sizes also imply that during impregnation first pores and then the external surface are coated.

Because of the small size of V_2O_5–K_2SO_4 particles, it was difficult to obtain the electron diffraction from as-prepared catalyst samples. However, under the action of the electron beam in the microscope, the particles showed a tendency to grow in size. Figures 4a and b show the electron micro-

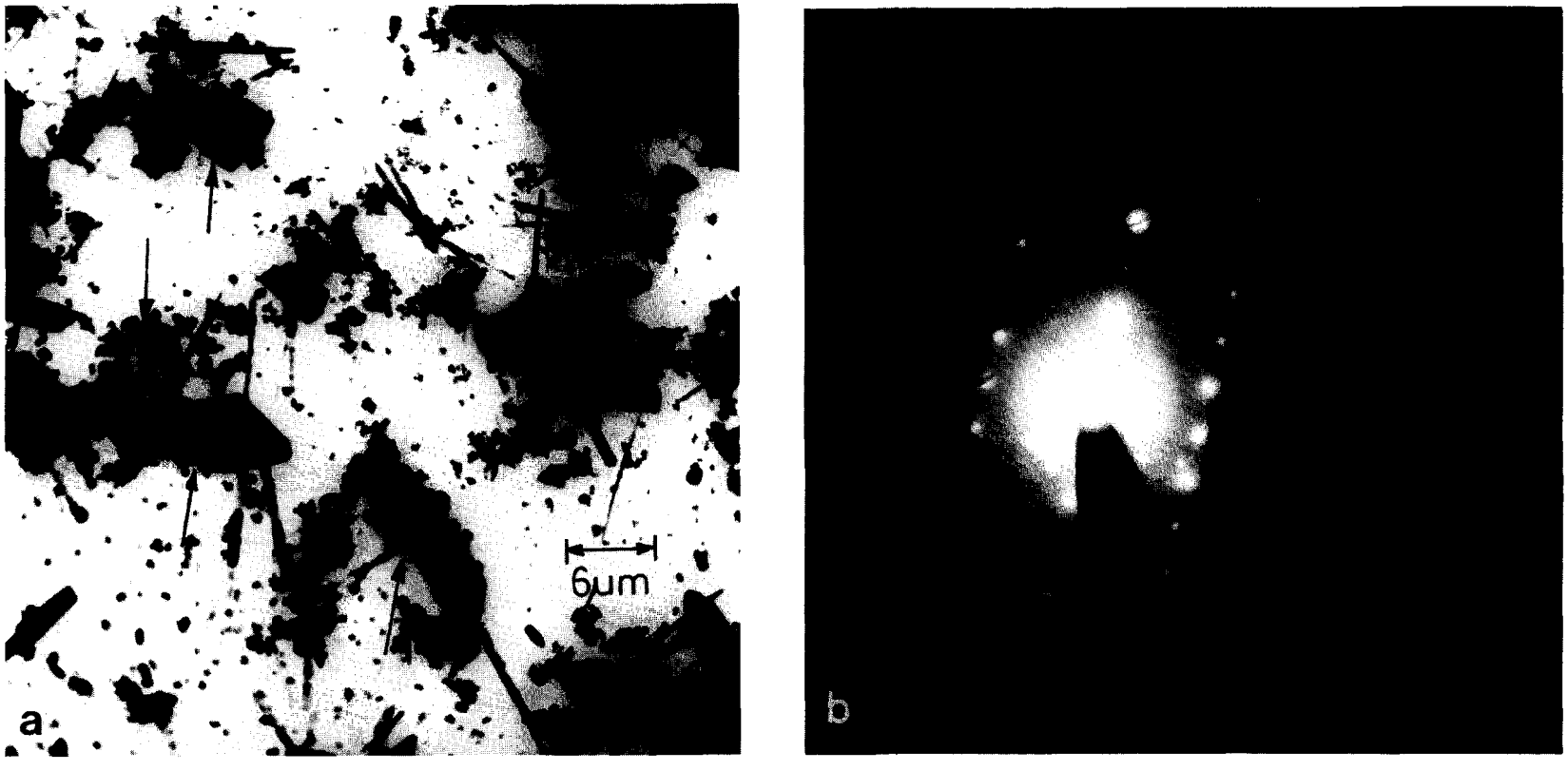

FIG. 1. Electron micrograph and diffraction pattern of V-20–K-15 catalyst showing V_2O_5 needles.

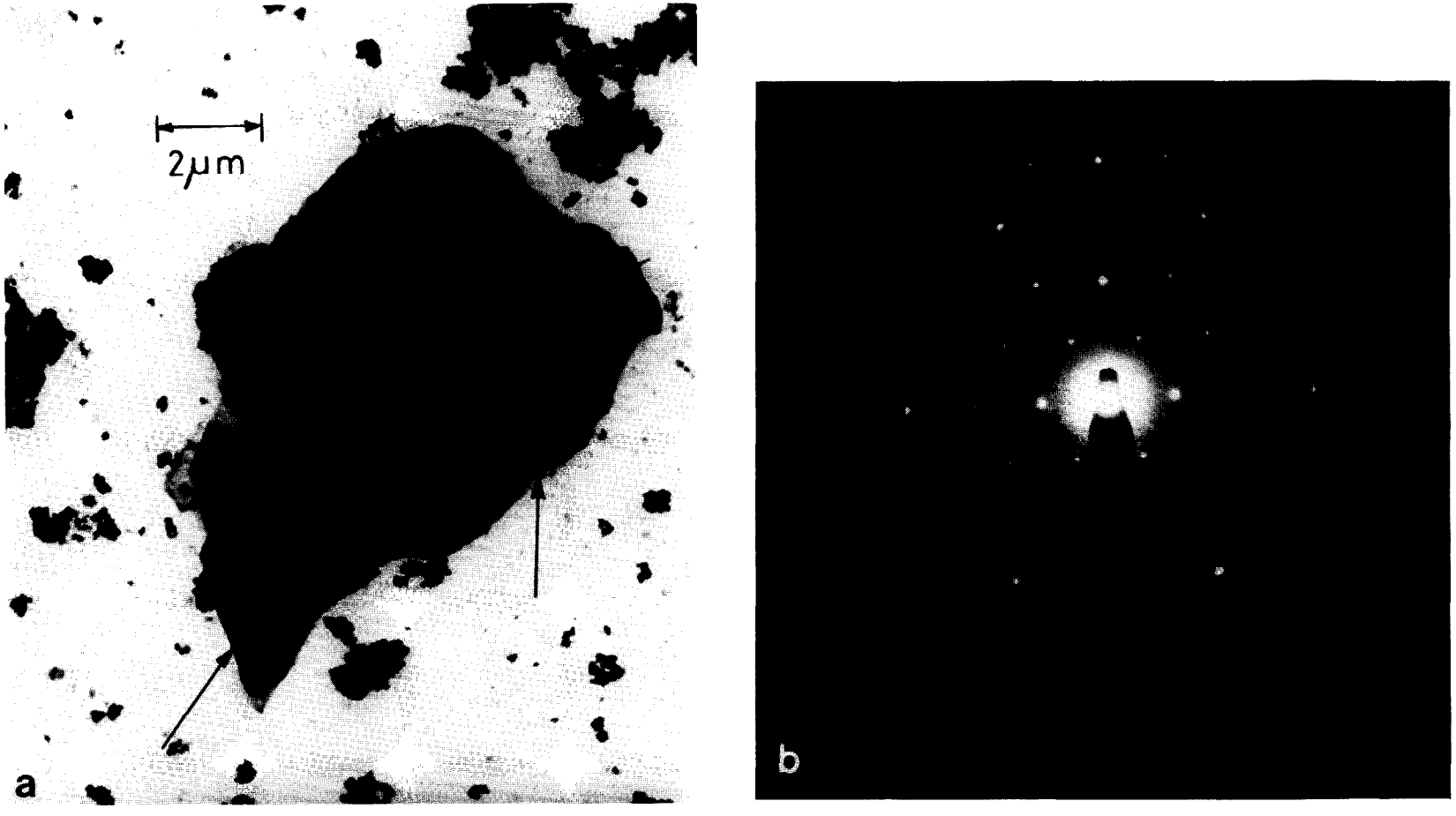

FIG. 2. Electron micrograph and diffraction pattern of V-15–K-20 catalyst showing K_2SO_4 platelet.

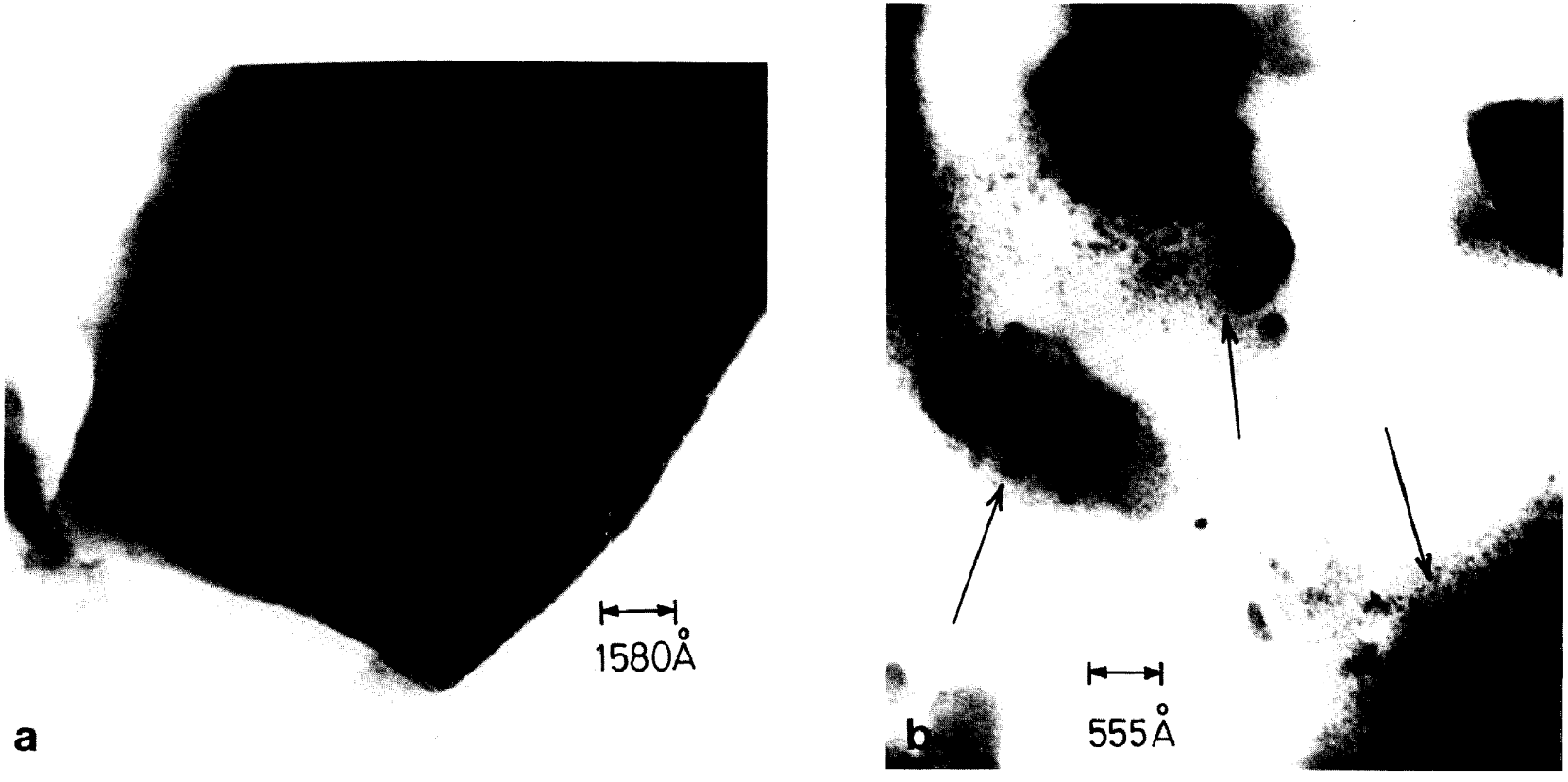

FIG. 3. Electron micrograph of V-20–K-10 catalyst showing (a) thick continuous coating of V_2O_5–K_2SO_4 on support grain, and (b) a fine dispersion of V_2O_5–K_2SO_4 particles on the support.

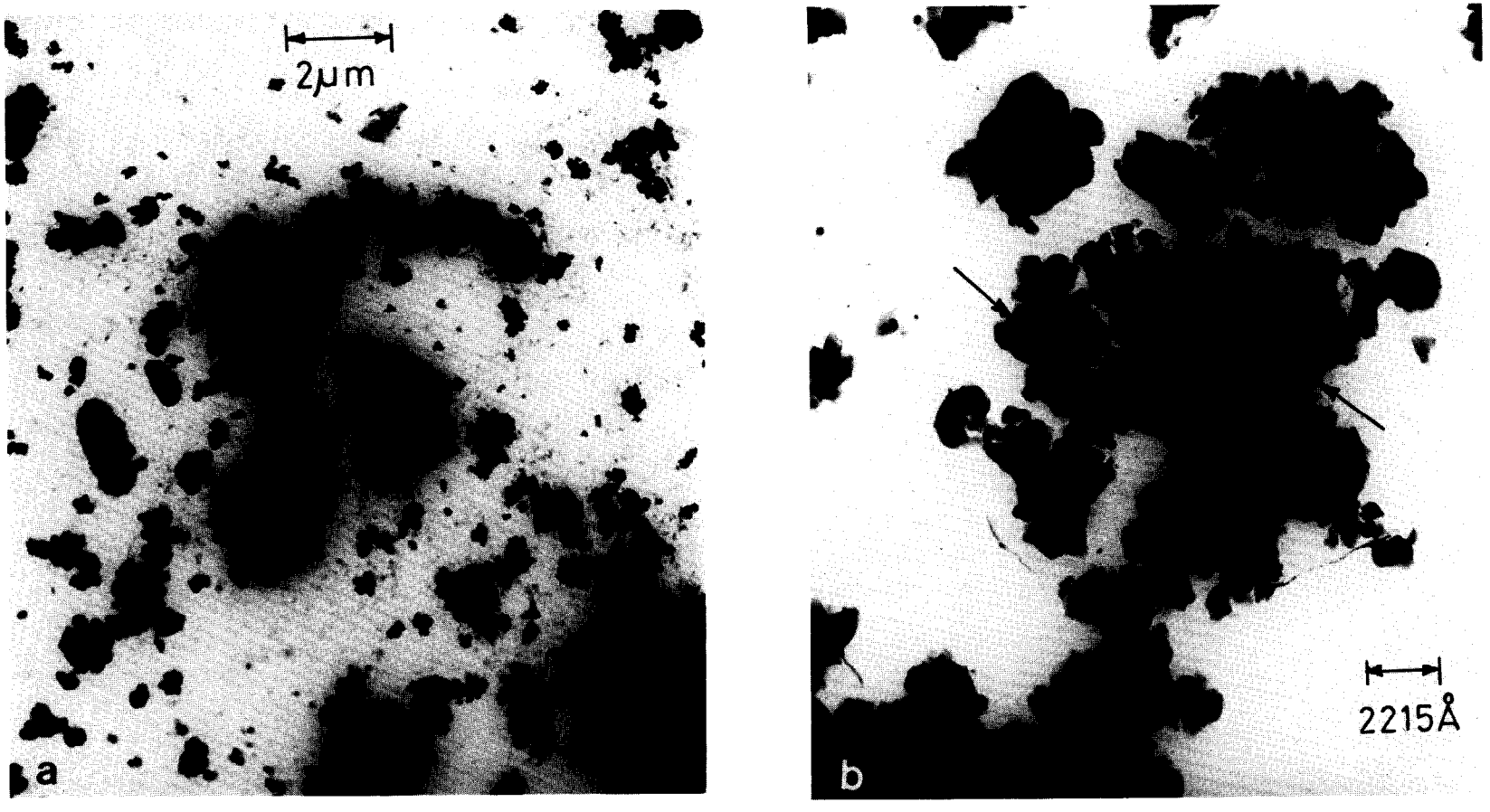

FIG. 4. Electron micrograph of V-15–K-20 catalyst (a) before and (b) after irradiation by the electron beam in the microscope and (c) diffraction pattern of irradiated particles.

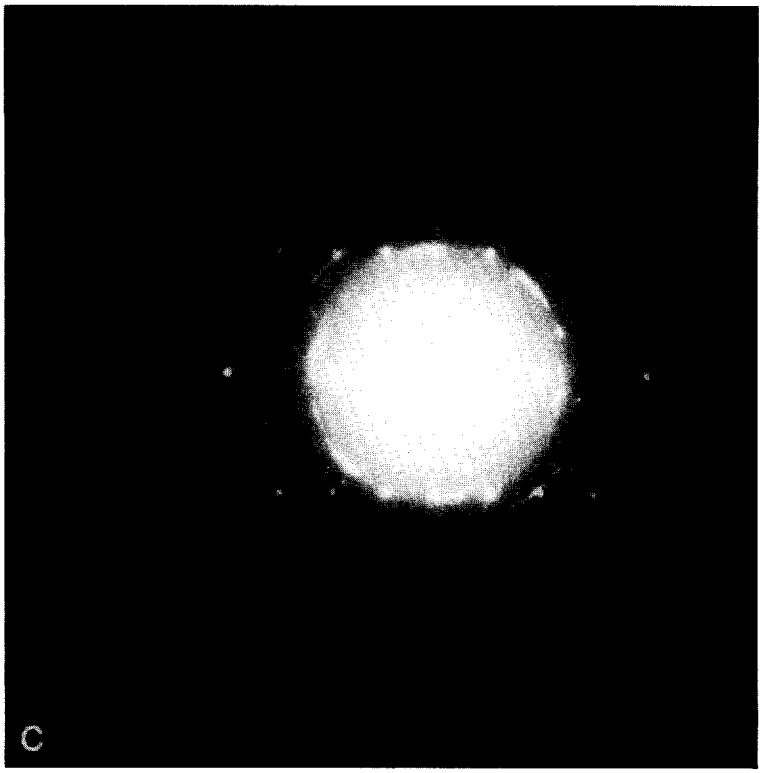

FIG. 4.—*Continued*

graphs of the V-15–K-20 catalyst sample before and after the irradiation. After their growth the particles exhibited a spotty-textured diffraction pattern as shown in Fig. 4c. Burzo *et al.* (*21*) in their studies on the V_2O_5–Fe_2O_3 system observed that under the action of the electron beam in the microscope some twins appear in the crystallites followed by the structural transformation of V_2O_5 to VO_x having an orthorhombic structure with parameters a = 8.1 Å, b = 10.4 Å, and c = 16.1 Å (*29, 30*). The diffraction pattern obtained in the present case does not seem to be indexicle on the basis of VO_x structure. It is probably that the Fe_2O_3 particles were present as molecular precipitates near the lattice defects and appeared in contrast in the electron microscope, similar to the VO_x phase.

Figure 5 shows the electron micrographs of catalyst samples with compositions V-20–K-10, V-20–K-15, and V-20–K-20. The corresponding particle size distributions for silica support particles impregnated with the active phase indicate that most of the particles were less than 1 μm size.

It appears that with 60-Å active-phase particles in the catalyst, the surface area should be much higher than reported in Table 1. However, it is to be noted that Figs. 3a and b are from the same catalyst. If the two figures are placed together on the same magnification scale, it is seen that the area over which active-phase particles are found as separate islands of about 60 Å forms a very small portion of the total area. The area fraction for this was, at a maximum, about 20%. The rest of the area is thickly coated with V_2O_5–K_2SO_4 resulting in a loss of support area. Thus, to ascertain the contribution of active-phase particles to the surface area it will be proper to take into account the fact that only a very small

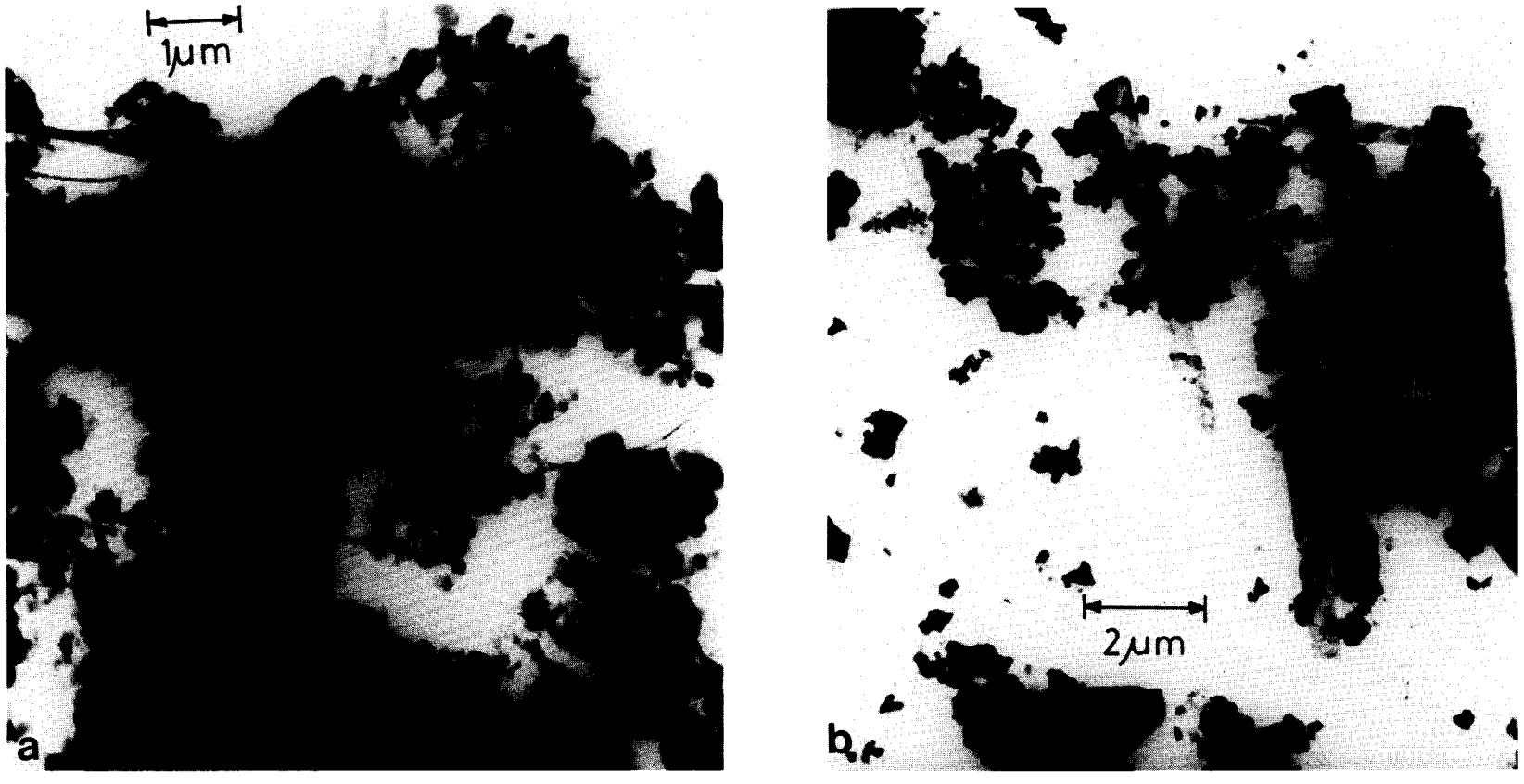

FIG. 5. Electron micrograph of (a) V-20–K-10, (b) V-20–K-15, and (c) V-20–K-20 catalyst.

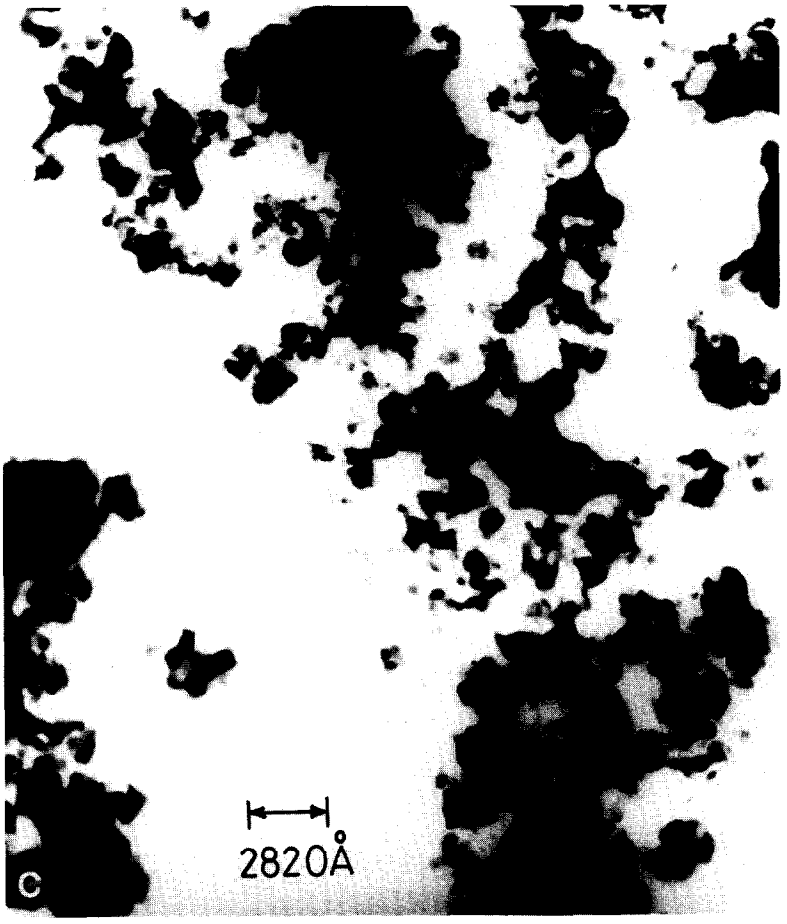

FIG. 5.—*Continued*

portion (5–20%) of the active phase remains well dispersed. Also, the silica particles contain pores with specific distribution. The surface areas of the different catalysts calculated on the basis of contribution of active-phase particles and silica support were found to be fairly close to the experimental values.

The physicochemical studies have shown that V_2O_5 and K_2SO_4 are finely dispersed over the carrier, without any interaction between them. This is in contrast to the results obtained by some workers (*1, 2, 25, 28*) who concluded that V_2O_5 is dissolved in a molten salt which closely resembles the composition of potasium pyrosulphate and also reported the presence of interaction products like $2\ V_2O_5 \cdot K_2O$ and $VOSO_4$ (*23*). However, such a comparison is not possible because the catalyst constituents and the preparation conditions were different. Whereas all the above authors studied unsupported V_2O_5–K_2SO_4 melt, the catalysts in the present investigations were silica supported and no melt was formed. Mars and Maessan (*4*) reported that in the asence of pyrosulphate, as in a V_2O_5–K_2SO_4 system, vanadium remains in the pentavalent state only.

B. Activity

Since one of the objectives of this work was to correlate the structural properties with the activity of the different catalysts, all other reaction parameters were kept constant. The catalytic activity was defined

as the number of moles of formaldehyde formed per mole of methanol fed. The experiments to investigate the effect of total active-phase concentration of the catalyst on the catalytic activity were conducted at a temperature of 400°C, with mole ratio $\bar{R}$ = 11% and W/F = 35 g hr/mole^{-1}. The total active-phase concentration ranged from 25 to 70 g per 100 g of the silica support. The activity increased rapidly with the amount of the active phase for concentrations up to about 55 g (V_2O_5 + K_2SO_4) per 100 g support and then started to decrease. The corresponding catalyst composition was V-20–K-15. The maximum activity was 84.5%.

Experiments were also carried out on catalysts with different K_2SO_4 to V_2O_5 weight ratios. Figure 6 shows the effect of K_2SO_4 concentration in the active phase on the catalytic activity for two different sets of experimental conditions; one for high conversion levels and the other for lower conversions. For both sets of experiments the activity is found to increase up to 65% of K_2SO_4 concentration. The maximum activity again corresponded to the catalyst composition V-20–K-15. Trama *et al.* (*25*)

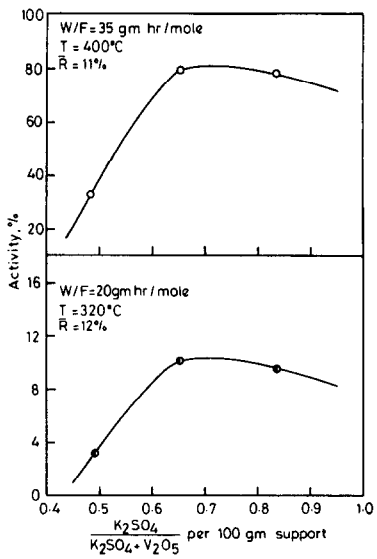

FIG. 6. Effect of K_2SO_4 concentration on the activity of the catalyst.

found the activity of the system for CO oxidation to be highest for K_2SO_4 concentration of 35% in the active phase.

There appears a close link between electron microscope observations and the activity of the catalysts. It was found that the proportion of needle-type V_2O_5 was different in all the catalyst samples, the highest being for the catalyst composition V-20–K-15. This indicates that the catalyst with the greater tendency to exhibit these needle structures has the higher activity. It has already been shown that the proportion of these needles depends on K_2SO_4 concentration. The promotioal action of K_2SO_4 may then be due to the growth of these V_2O_5 needles which provide a large number of highly active centers (*26*).

If attention is focused on the BET results (Table 1), it is evident that with the increase in V_2O_5 concentration the surface area, pore volume, and porosity decrease but the value of average pore radius increases. With the increase in K_2SO_4 concentration, pore volume and porosity decrease but the surface area passes through minimum. Also, average pore radius first increases and then decreases. These observations are similar to those of Castellan *et al.* (*32*) who found that at certain compositions more micropores are formed than are originally present in the support, resulting in an increase in the surface area. There is an optimum value of K_2SO_4 concentration at which both the surface area and the pore radius are optimum. This corresponded to V-20–K-15 where the maximum activity was obtained.

C. Spent Catalyst

To get an idea of the changes in morphology and the microstructure of the catalyst after catalysis, a catalyst (V-20–K-15) used for about 50 runs was studied using X-ray and electron microscopy. The X-ray diffraction from the spent catalyst indicated all the lines characteristic for the fresh catalyst. Thus, all the components present

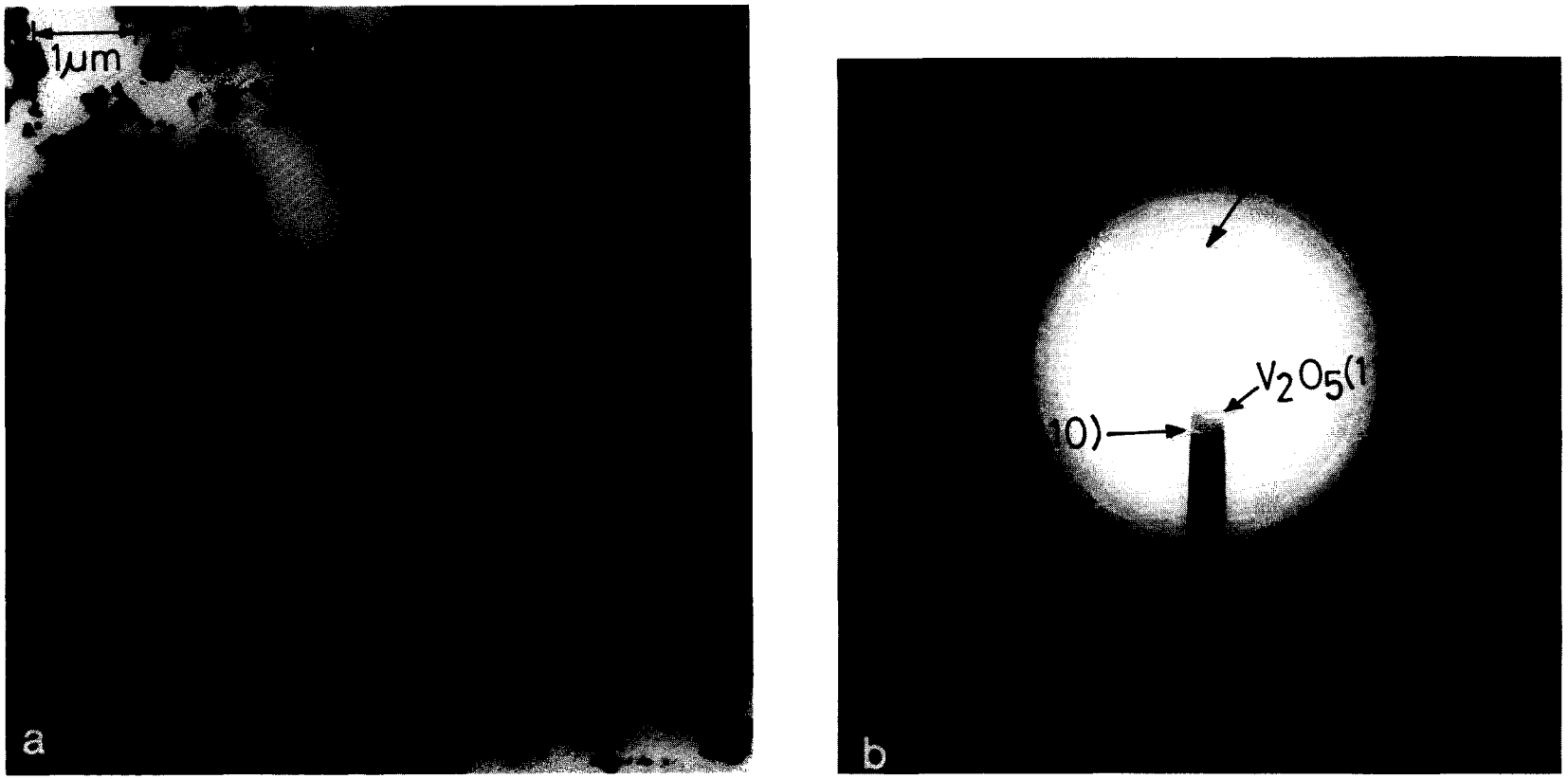

FIG. 7. Electron micrograph and diffraction pattern of a spent V-20–K-15 catalyst.

in the fresh catalyst remained unchanged after the catalysis. The microstructure of the catalyst, however, showed small changes. The long-needle structures seemed to be partially disintegrated. The micrograph and the electron diffraction pattern from such a catalyst sample are shown in Fig. 7. The pattern was found to be indexicle on the basis of orthorhombic V_2O_5 and hexagonal K_2SO_4. The average particle size was also found to decrease from 1 to 0.65 μm. The activity for such a spent catalyst was about 15% less than that for a fresh catalyst. The studies indicated that the V_2O_5 needles might act as centers of high activity and such needles and other large particles partially disintegrated during catalysis over extended runs leading to a structure of small grains.

APPENDIX: NOTATION

a, b, c	Unit cell parameters (Å)
d	Interplanar spacing (Å)
θ	Bragg's angle (in degrees)
W	Weight of the catalyst (g)
F	Molar feed rate (mole/hr)
T	Temperature
$\bar{R}$	Mole ratio of methanol to air in the feed mixture
$\bar{r}$	Mean pore radius (Å)
V_p	Pore volume (cm^3/g)
$S.A.$	Surfae area (m^2/g)

REFERENCES

1. Kiyoura, R., *Science (Japan)* **10,** 126 (1940); *Chem. Abs.* **34,** 7169 (1940).
2. Fraser, J. H., and Kirkpatrick, W. J., *J. Amer. Chem. Soc.* **62,** 1659 (1940).
3. Boreskov, G. K., and Pligunov, V. P., *J. Appl. Chem. USSR* **13,** 653 (1940).
4. Mars, P., and Maessen, J. G. H., *in* "Proceedings, 3rd International Congress on Catalysis, Amsterdam, 1964," Vol. 1, p. 266. Wiley, New York, 1965.
5. Bhattacharya, S. K., Janikiram, K., and Ganguli, N. D., *J. Catal.* **8,** 128 (1967).
6. August, G., *Neth. Appl.* **6,** 410, 777 (1965); *Chem. Abs.* **63,** 11434g (1966).
7. Fakuda, T., *J. Chem. Soc. Japan Ind. Chem. Sect.* **54,** 111 (1951); *Chem. Abs.* **47,** 4844 (1953).
8. Margolis, L. Y., and Plyshevaskaya, E. G., *Izvest. Akad. Nauk SSR,* 697 (1953); *Chem. Abs.* **50,** 14523 (1956).
9. Mann, R. S., and Dosi, M. K., *J. Catal.* **28,** 282 (1973).
10. Malinski, R., Akimoto, M., and Echigoya, E., *J. Catal.* **44,** 101 (1976).
11. Tandy, G. H., *J. Appl. Chem.* **6,** 68 (1956).
12. Krupay, B. W., and Ross, R. A., *J. Catal.* **50,** 220 (1977).
13. Bibin, V. N., and Kasatkina, L. A., *Kinet. Catal.* **15,** 653 (1964).
14. Boreskov, G. K., "Catalysis in Sulfuric Acid Production" (in Russian). State Press for Chemical Literature, Moscow, 1954.
15. Dzisyak, A. P., Boreskov, G. K., Kasatkina, L. A., and Kochurikhin, V. E., *Kinet. Catal.* **2,** 727 (1961).
16. Jiru, P., Tomkova, D., Jara, V., and Wankova, J., *Z. Anorg. Allg. Chem.* **121,** 303 (1960).
17. Franklin, N. L., Pinchebeck, P. H., and Popper, F., *Trans. Inst. Chem. Eng.* **34,** 280 (1956).
18. Pinchbeck, P. H., *Chem. Eng. Sci.* **6,** 105 (1957).
19. Agarwal, D. C., Nigam, P. C., and Srivastava, R. D., *J. Catal.* **55,** 1 (1978).
20. Clark, H., and Berets, D. G., *Proc. Inst. Congr. Catal.* **1,** 204 (1956).
21. Burzo, E., Stanescu, L., and Teodorescu, V., *J. Mat. Sci.* **13,** 1855 (1978).
22. Grymonprez, G., Fierman, S. L., and Vennik. *J. Acta Cryst. A* **33,** 834 (1977).
23. Kiyoura, R., *Ryusan* **2,** 253, 287 (1949).
24. Trama, K., Teranishi, S., Yoshida, S., and Yoshida, H., *Bull. Chem. Soc. Japan* **34,** 1185 (1961).
25. Trama, K., Teranishi, S., Yoshida, S., and Tamura, N., *in* "Proceedings, 3rd International Congress on Catalysis, Amsterdam, 1964," Vol. 1, p. 282. Wiley, New York, 1965.
26. Hassan, S. A., and Iskandar, F. T., *J. Catal.* **43,** 242 (1976).
27. Athappan, R., Thesis, Indian Institute of Technology, Kanpur, 1979.
28. Illarionov, V. V., *Zhur. Neorg. Khim.* **1,** 780 (1956).
29. Tilley, R. J. D., and Hyde, B. G., *J. Phys. Chem. Solids* **31,** 1613 (1970).
30. Hyde, B. G., and Tilley, R. J. D., *Phys. Status Solidi A* **2,** 749 (1970).
31. Chatelier, H. L., *Bull. Soc. Min* **47,** 300 (1887); Mellor, J. W., Comp. Treatise *Inorg. Theoret. Chem.* **2,** 662 (1956).
32. Castellan, A., Bart, J. C. J., Vaghi, A., and Giordano, N., *J. Catal.* **42,** 162 (1976).